EVALUATION OF MODIFIED k - ε MODELS IN SIMULATING 3D FLOWS OVER SUBMERGED SPUR DIKES

Jing Peng
Department of Hydraulics, China Institute of Water Resources and Hydropower Research
1A Fuxing Road, Beijing 100038, CHINA

Yoshihisa Kawahara
River Department, Public Works Research Institute, Ministry of Construction
Asahi 1, Tsukuba, Ibaraki 305-0804, JAPAN

Guangwei Huang
Department of Civil Engineering, The University of Tokyo
Hongo, Bunkyo-ku, Tokyo 113-8656, JAPAN

ABSTRACT

A three-dimensional numerical model incorporating a k-ε type of turbulence model was developed for flows in open channels with submerged spur dikes. The applicability of the standard k-ε model, three modified linear models and a nonlinear model were tested for two different flows. Comparison among these models with the experiments showed that the modified k-ε models reproduce the turbulence quantities better than the standard model and that the nonlinear model can achieve more accurate predictions. The superiority of the nonlinear model over the linear models is attributed to its more accurate approximation of Reynolds stresses, and hence improved calculation of turbulent eddy viscosity around spur dikes.

INTRODUCTION

Spur dikes along riverbanks have been constructed to protect riverbank from erosion at high water depth or to control riverbed topography for navigation at low water situation. Recently they have also been used to enhance aquatic habitat by providing diverse flow environment. Fundamental research on flow and sediment transport around spur dikes is indispensable to fully understand the complex transport processes and hence to develop the methodology for spur dike design.

Due to the difficulties in measuring flood flow, the CFD approach has been increasingly utilized to analyze the flow feature. But the flow around spur dikes involves so many complex phenomena, such as separation, recirculation, curved shear layer, high turbulence level and moving boundaries, that the numerical simulation requires more advanced flow modeling and numerical techniques.

One of the main difficulties in simulating this kind of flow is the performance of turbulence models. It is well known that the standard k-ε model underpredicts the size of recirculation zone around bluff bodies through the overestimation of turbulence production rate and consequently the magnitude of eddy viscosity near bluff bodies. A lot of efforts have been made to improve the prediction of the standard k-ε model in simulating flows with separation.

In this study, several modified k-ε type turbulence models are tested in two cases: 1) flow around an isolated submerged spur dike and 2) flow around spur dikes installed in series. In what follows, firstly all the models are applied to the flow with an isolated spur dike to compare the model performances against the experimental data. Then selected models are further tested in CASE-2 where spur dikes in series mimic the practical situation more reasonably.

NUMERICAL MODELS

Basic Equations

The basic equations solved here are the continuity equation, three momentum equations and the transport equations of turbulence energy and its dissipation rate. They are expressed as follows.

$$\frac{\partial U_i}{\partial x_i} = 0 \tag{1}$$

$$\frac{\partial U_i U_j}{\partial x_j} = -\frac{1}{\rho}\frac{\partial}{\partial x_i}\left(P + \rho g Z_b\right) + \frac{\partial}{\partial x_i}\left(\nu \frac{\partial U_i}{\partial x_j} - \overline{u_i u_j}\right) \tag{2}$$

$$\frac{\partial U_i k}{\partial x_i} = \frac{\partial}{\partial x_i}\left[\left(\nu + \frac{\nu_t}{\sigma_k}\right)\frac{\partial k}{\partial x_i}\right] + P_{rod} - \varepsilon \tag{3}$$

$$\frac{\partial U_i \varepsilon}{\partial x_i} = \frac{\partial}{\partial x_i}\left[\left(\nu + \frac{\nu_t}{\sigma_\varepsilon}\right)\frac{\partial \varepsilon}{\partial x_i}\right] + \frac{\varepsilon}{k}\left(c_{\varepsilon 1} P_{rod} - c_{\varepsilon 2}\varepsilon\right) \tag{4}$$

$$P_{rod} = -\overline{u_i u_j}\frac{\partial U_i}{\partial x_j} \tag{5}$$

where U_i is the mean velocity, P the pressure, Z_b the bed level, k the turbulence energy, ε the dissipation rate and ν_t the eddy viscosity.

Turbulence Models

The turbulence models discussed here are four linear models and a nonlinear model. The Reynolds stresses in linear models are expressed using the eddy viscosity as:

$$-\overline{u_i u_j} = 2\nu_t S_{ij} - \frac{2}{3}k\delta_{ij} \tag{6}$$

$$S_{ij} = \frac{1}{2}\left(\frac{\partial U_i}{\partial x_j} + \frac{\partial U_j}{\partial x_i}\right) \tag{7}$$

Each model is proposed based on its modeling principle, which results in the different model coefficients.

Standard model

$$c_\mu = 0.09,\ c_{\varepsilon 1} = 1.42,\ c_{\varepsilon 2} = 1.92,\ \sigma_k = 1.4,\ \sigma_\varepsilon = 1.3 \tag{8}$$

RNG model by Speziale-Thangam (1992)

$$c_\mu = 0.085,\ c_{\varepsilon 1} = 1.42 - \frac{\eta(1-\eta/4.38)}{1+0.015\eta^3},\ c_{\varepsilon 2} = 1.68, \tag{9}$$

$$\sigma_k = \sigma_\varepsilon = 1.3 \tag{10}$$

$$\eta = Sk/\varepsilon,\ S = (2S_{ij}S_{ij})^{1/2} \tag{11}$$

Launder-Kato model(1993) (LK)

$$P_{rod} = \nu_t S\Omega,\ \Omega = (2\Omega_{ij}\Omega_{ij})^{1/2},\ \Omega_{ij} = \frac{1}{2}\left(\frac{\partial U_i}{\partial x_j} - \frac{\partial U_j}{\partial x_i}\right) \tag{12}$$

Zhu-Shih model(1994)

$$c_\mu = \frac{2/3}{5.5+\eta},\ c_{\varepsilon 1} = 1.42,\ c_{\varepsilon 2} = 1.92,\ \sigma_k = 1.4,\ \sigma_\varepsilon = 1.3 \tag{13}$$

Nonlinear model by Shih et al.(1995)

$$\overline{u_i u_j} = \frac{2}{3}k\delta_{ij} - C_\mu\frac{k^2}{\varepsilon}2S^*_{ij} + 2C_2\frac{k^3}{\varepsilon^2}(-S^*_{ik}\Omega^*_{kj} + \Omega^*_{ik}S^*_{kj}) \tag{14}$$

$$C_\mu = \frac{1}{6.5+A^*_s U^*_s (k/\varepsilon)},\quad C_2 = \frac{\sqrt{1-9C^2_\mu (S^*(k/\varepsilon))^2}}{1+6S^*\Omega^*(k^2/\varepsilon^2)} \tag{15}$$

$$S^* = \sqrt{S^*_{ij}S^*_{ij}},\quad \Omega^* = \sqrt{\Omega^*_{ij}\Omega^*_{ij}}, \tag{16}$$

$$U^* = \sqrt{S^*_{ij}S^*_{ij} + \Omega^*_{ij}\Omega^*_{ij}},\quad W^* = \frac{S^*_{ij}S^*_{jk}S^*_{ki}}{(S^*)^3}, \tag{17}$$

$$S^*_{ij} = S_{ij} - \frac{1}{3}S_{kk\,ij},\ \Omega^*_{ij} = \Omega_{ij} \tag{18}$$

$$A^*_s = \sqrt{6}\cos\phi_1,\ \phi_1 = \frac{1}{3}\arccos(\sqrt{6}W^*) \tag{19}$$

$$c_{\varepsilon 1} = 1.42,\ c_{\varepsilon 2} = 1.92,\ \sigma_k = 1.0,\ \sigma_\varepsilon = 1.3 \tag{20}$$

Numerical Method

The basic equations were discretized by the finite volume method and were solved using the SIMPLE algorithm. A stabilized QUICK scheme proposed by Hayase et al.(1992) was utilized for the accurate discretization of convection terms. Preconditioned conjugate gradient-like solvers were applied to the sets of linearlized discretized equations.

Boundary conditions were given at inlet, outlet, free surface and wall boundaries. The velocity components and turbulence quantities were specified at inlet. At the downstream end, the longitudinal gradients of all the variables were assumed to be zero. Free surface was treated as a symmetry plane. Along wall boundaries including bed and sidewalls of the channel and all the spur dike faces, the wall function approach was used to reduce the total computational time.

COMPARISON OF TURBULENCE MODELS

Case-1 : Isolated Spur Dike

Five turbulence models are applied to the flow around an isolated submerged spur dike. The experimental data are reported by Tominaga and Chiba (1996). The geometry of the flow domain is schematically shown in Fig. 1. The x-coordinate is aligned in the streamwise direction, y-coordinate in the spanwise direction and z-coordinate in the vertical direction. An isolated spur dike is located at x = 4m from the flume entrance. Flow discharge is 3,600cm^3/s with a water depth of 9cm with small fluctuation of free surface.

Numerical simulations are carried out on the grid system that has 147×47×20 nodal points. In the following discussions, all the quantities in the figures are normalized by the upstream mean velocity u_m, when they are not specially mentioned.

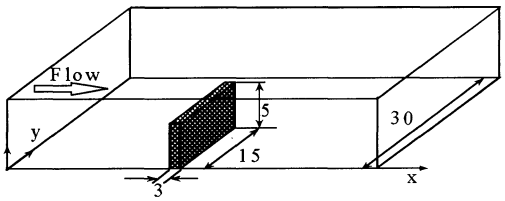

Figure 1. Flow over a submerged spur dike (unit: cm).

Fig. 2 compares the streamwise velocity profiles at two locations. In Fig. 2 (a), velocity distributions predicted by all the models near bed are generally close, except in the regions near opposite side bank (y>0.25m) and behind the spur dike (y<0.10m). Reverse flow exists at the backside of the spur dike. Prediction by the nonlinear model shows the best agreement with the measured data although it seems to predict stronger reverse flow than the experiment, giving larger negative value around y=0.06m. It is noted that all the models slightly overestimate the velocity at the tip region of spur dike (around y=0.15m).

Fig. 2 (b) shows the velocity profiles near free surface. The differences among the models are apparent at the center of the flume. The standard model, Launder-Kato model and Zhu-Shih model considerably overestimate the measured

data. The RNG model slightly overestimates the magnitude of velocity, while the nonlinear model gives closest result with the experiment.

Fig. 3(a), (b) and (c) show the measured u-v vectors near the bed wall (in the horizontal plane of 2cm above the bed) and the calculated results by Zhu-Shih model and the nonlinear model as examples. Recirculating flow pattern behind the spur dike is reasonably reproduced by these models. The experiment reports the reattachment length behind the spur dike about 0.7 L_g (where L_g is the length of spur dike in spanwise direction). Zhu-Shih model and nonlinear model predict the reattachment length as $1.0L_g$ and $0.8L_g$ respectively, both overpredicting this parameter to some degree.

Fig.4 shows the bed shear stress distribution (expressed by friction coefficient $C_f^+ = \tau_b / 0.5\rho u_m^2 \times 10^3$) around a spur dike by all the models. It can be seen that the main variance in the contour lines occurs in the tip part of the spur dike. The standard k-ε model gives wide spread of high value (for example the contour line of $C_f^+ = 26$) in the tip region. This high level region is reduced in the results by the other models. It is well recognized that the standard k-ε model overpredicts the production of turbulence energy in the vicinity of stagnation point, which essentially cause the overestimation of the bed shear stress. In this flow around a spur dike there is a stagnant point just in the tip part. The comparison in Fig. 4 confirmed indirectly the overprediction of the turbulence energy by the standard k-ε model and, at the same time, the improved performance by all the other models.

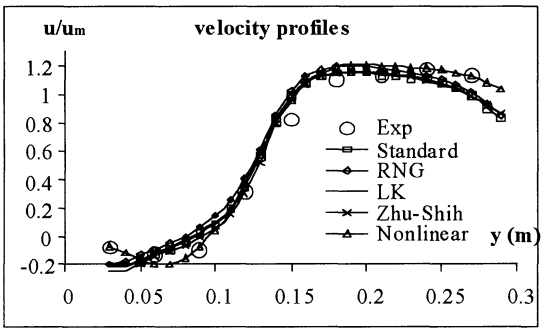

(a) At x=4.1m, z=1.0cm.

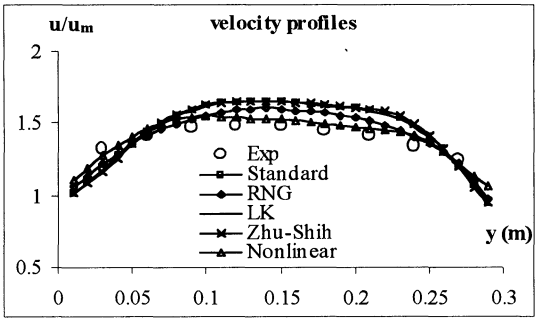

(b) At x=4.0m, z=7.0cm.

Figure 2. Velocity profiles by various turbulence models.

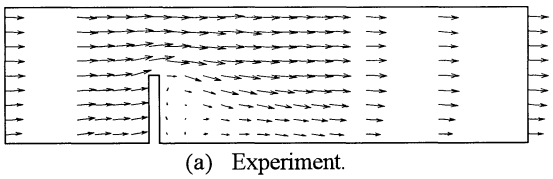

(a) Experiment.

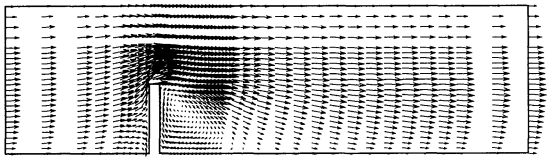

(b) Zhu-Shih model.

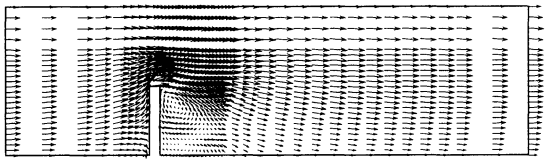

(c) Nonlinear model.

Figure 3. Velocity vectors in horizontal plane (2cm above bed).

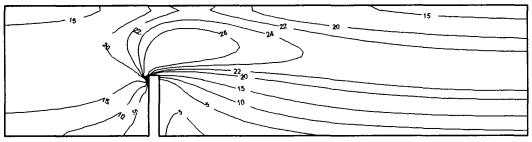

(a) Standard model.

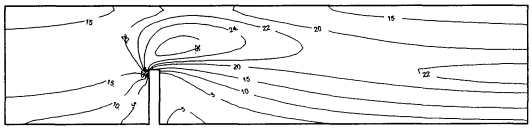

(b) RNG model.

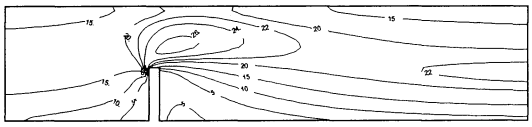

(d) LK model.

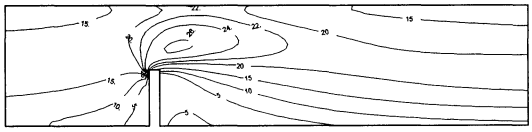

(e) Zhu-Shih model.

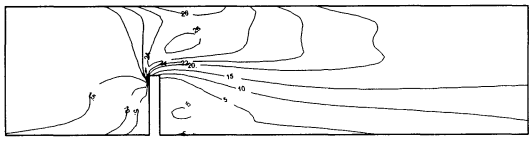

(f) Nonlinear model.

Figure 4. Bed shear stress distribution.

The overestimation of the turbulence level by the standard k-ε model can be traced back to the different level of the turbulent eddy viscosity in the separation and recirculation zones. Fig. 5 compares the distribution of eddy viscosity ν_t near bed along transverse line right behind the spur dike. Here ν_t is normalized as $\nu_t^+ = \nu_t / u_m h \times 100$, h being the height of the spur dike. The magnitude of eddy viscosity varies according to different models. In the recirculation zone (y<0.15m) the standard k-ε model predicts the highest level of eddy viscosity. Lower level is given by the RNG and Launder-Kato models, and much more reduction of the eddy viscosity is obtained by the Zhu-Shih and the nonlinear models. At the tip region near the spur dike where separation prevails, modified models, especially Zhu-Shih and the nonlinear models, effectively increase the value of ν_t. Local variation in ν_t contributes to the improvement in their predictive behaviors.

From these comparisons it can be said that modified linear k-ε models, particularly Zhu-Shih model and RNG model can predict the flowfield better than the standard model and that more accurate prediction can be achieved by the nonlinear model.

In the next case, Zhu-Shih model out of linear models and the nonlinear model are further tested.

Case-2 : Submerged Spur Dikes in Series

In many practices, spur dikes are not installed in an isolated way but are arranged in series to function as a spur dike system for efficient riverbank protection. The flow structure and sediment transport phenomena become more complicated under this situation because of the interaction of spur dikes.

The experiment is carried out in a flume of 10m long and 0.6m wide. Spur dikes of the same size (3×10×5 cm^3) are installed along a side bank at constant interval. Measuring section is placed at downstream reach of the flume where the flow is fully developed. Fig. 6 shows the measuring section between two spur dikes and the arrangement of the coordinate system in the numerical simulation. The location of the first spur dike in the measuring section is at x=0~3cm, y=0~10cm and z=0~5cm. The flow discharge is 21,300cm^3 /s with the water depth of around 8.0cm in the central part of the flume. The results with the spur dike interval of 40cm are compared with the numerical ones.

Fig. 7 (a) and (b) give the longitudinal velocity profile along the spanwise axis 1cm away from the bed. The section x=8.0cm locates in the recirculation region behind the spur dike. The comparison shows that Zhu-Shih model overpredicts the velocity in the tip region of spur dikes (around y=10~20cm) while the nonlinear model shows good agreement with the experiment. The two models, however, underestimate the velocity near the opposite side wall and miss the peak value in this region (around y=40~60cm) observed in the experiment.

Streamwise velocity profiles along the spanwise axis 5cm above the bed (same height with the spur dike top surface) are shown in Fig. 8 (a) and (b). It again shows that the linear model largely overestimates the velocity in the center part of the flume. The nonlinear model improves the prediction in this region, although it underestimates the velocity behind the spur dike. The peak value of the velocity

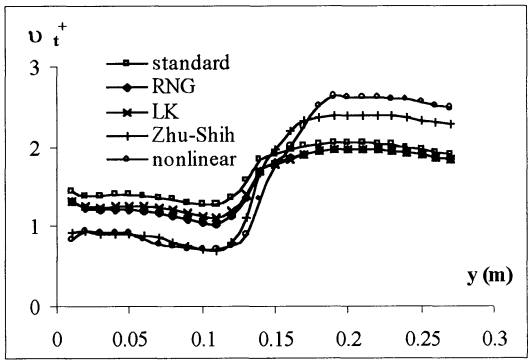

Figure 5. Eddy viscosity distribution.

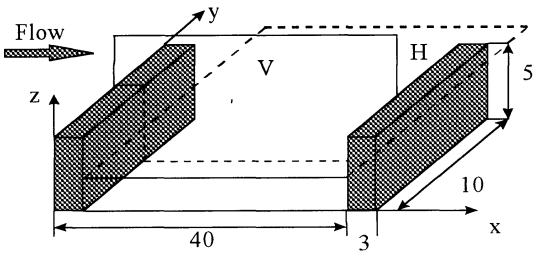

Figure 6. Flow over spur dikes in series (unit: cm).

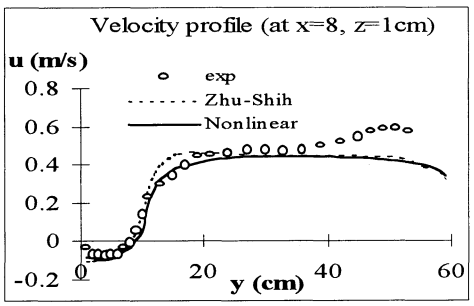

(a) At x=8cm.

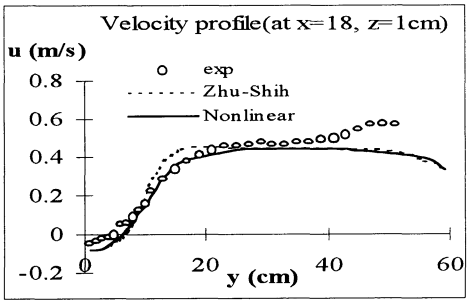

(b) At x=18cm.

Figure 7. Streamwise mean velocity profiles (1cm above bed).

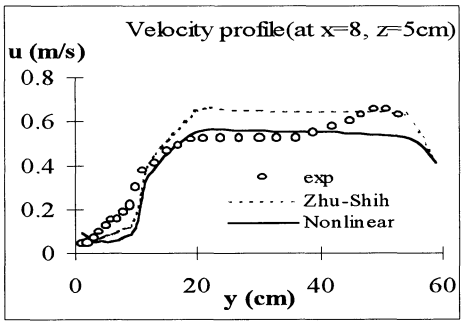

(a) At x=8cm.

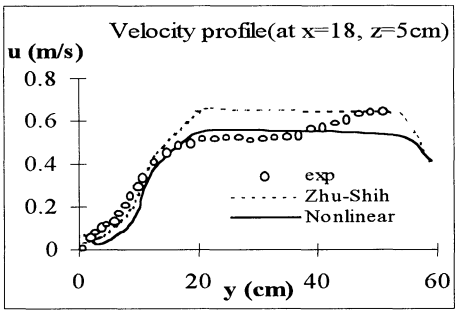

(b) At x=18cm.

Figure 8. Streamwise mean velocity profiles (5cm above bed).

near the opposite sidewall is not well captured by the two models, whose reason still remains unclear.

These figures demonstrate that the nonlinear model reproduces the flow pattern better than Zhu-Shih model. The improvement by the nonlinear model can also be confirmed in the u-v vectors. Fig. 9 depicts the plan view of u-v velocity distribution near the bed in spur dike region. The experiment shows that the flow directs from the spur dike region towards the channel center with recirculation zones. The complex flow pattern is reasonably captured by the nonlinear model.

The side wiew of v-w vectors in the vertical plane away from free surface are given in Fig. 10. It shows the formation of primary recirculation behind the spur dike although it has slight difference in flow direction. Zhu-Shih model slightly overpredicts the size of recirculation zone. The nonlinear model offers better agreement with the experiment in both the size and the location of recirculation zone.

To further discuss the reasons why the nonlinear model improves the predictions particularly in the tip part of spur dikes, the distributions of turbulent kinetic energy and eddy viscosity are illustrated to analyze their effects on the mean flowfield. Fig. 11 compares the dimensionless ν_t and k profiles by the two numerical models along the same spanwise line as in Fig. 7. The quantities of ν_t and k are normalized by the height of spur dike h and the upstream mean velocity u_m as: $\nu_t^+=100\cdot\nu_t/hu_m$, $k^+=100\cdot k/u_m^2$. Fig. 11 (a) presents the profiles of ν_t, where the nonlinear model gives reduced value of ν_t in the region near the spur dikes

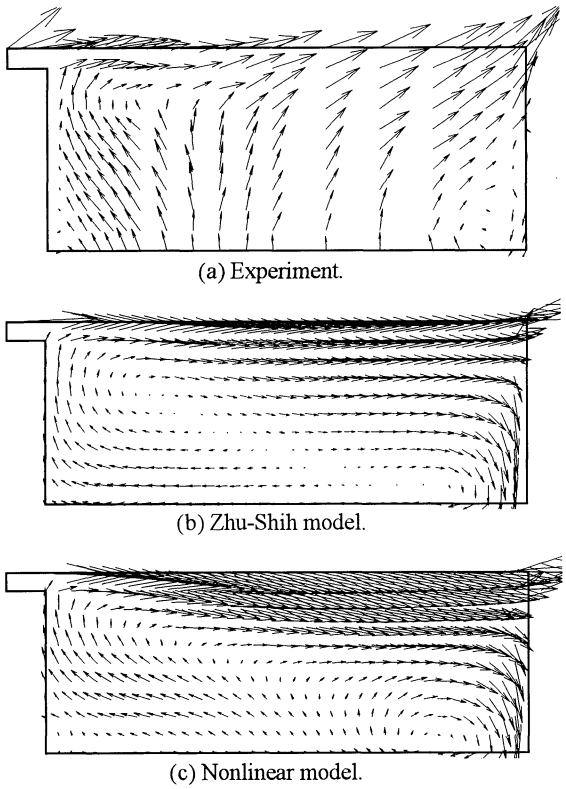

(a) Experiment.

(b) Zhu-Shih model.

(c) Nonlinear model.

Figure 9. U-V vector distribution (z=1cm above bed).

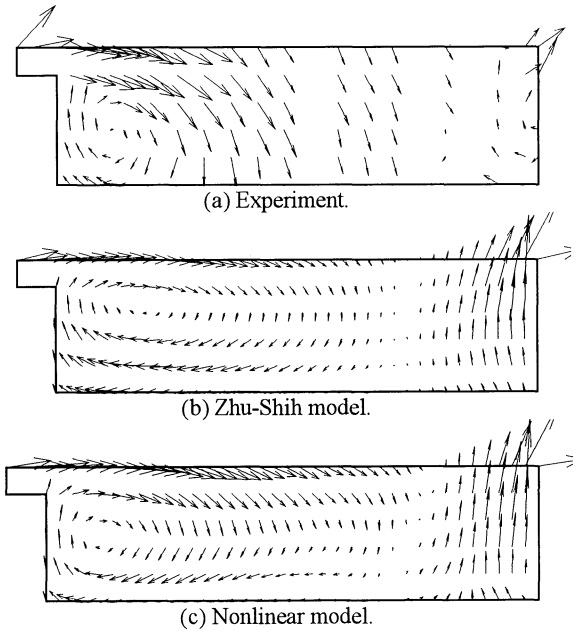

(a) Experiment.

(b) Zhu-Shih model.

(c) Nonlinear model.

Figure 10. U-W vector distribution (y=1cm from side).

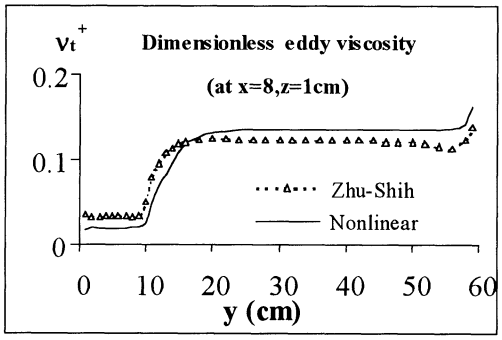

(a) Eddy viscosity.

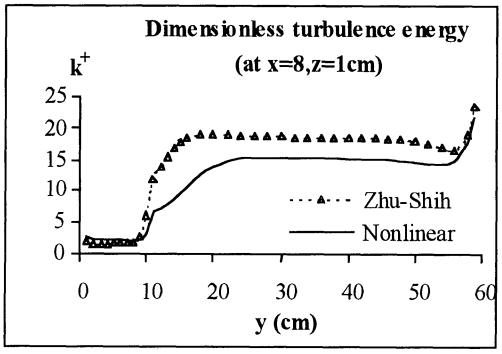

(b) Turbulence energy.

Figure 11. Non-dimensional tubulent quantities.

(y<20cm) and increased level of ν_t in the region away from the spur dikes. The variation in ν_t by the nonlinear model is larger than that by Zhu-Shih model.

The non-dimensional turbulence energy shown in Fig. 11 indicates that Zhu-Shih model yields a rapid increase in turbulence energy in the tip region (y=10cm~20cm) with keeping higher level of k in the other part. On the other hand the nonlinear model gives a lower level of turbulence energy with a relatively smooth increase of k in the tip region. It is indicated that the overprediction of streamwise mean velocity by Zhu-Shih model is due to the overestimation of turbulence quantities such as the turbulent eddy viscosity ν_t and energy k.

CONCLUDING REMARKS

A numerical model is developed using a turbulence model to analyze the flows in rivers with submerged spur dikes. Since the turbulence model exerts significant influence over the predicted flowfield with separation and recirculation around spur dikes, it is necessary to scrutinize the performance of the turbulence model. In this study five k-ε type of models are selected based on the computational burden and their applicability to natural rivers of complex shape and are compared against two sets of experimental data. The turbulence models examined the standard k-ε model, a RNG model by Speziale-Thangam, Launder-Kato model, a Zhu-Shih model which are linear k-ε models and a nonlinear one by Shih et al. Through the comparisons about the distributions of mean velocities, bed shear stress, turbulence energy and eddy viscosity, the following results are drawn.

(1) The modified k-ε models can predict the velocity distribution and bed shear stress more reasonably than the standard k-ε model. Out of linear models, Zhu-Shih model and RNG model reproduce somehow better than the other models.
(2) The nonlinear model can offer more accurate velocity distribution than the linear models. Hence this model is recommended irrespective of the additional computational cost.
(3) The superiority of the nonlinear model over the linear models is attributed to its more accurate approximation of Reynolds stresses, eddy viscosity around the spur dikes.
(4) Although the model performance is made clear, all the models underpredict the velocity in the tip region of the spur dike and near the opposite sidewall of the spur dikes in series.
(5) Further research is necessary to reproduce the vortex shedding phenomenon at the tip part and to capture the spatial and temporal variation of free surface around spur dikes, in particular when the water surface is not so high compared with the height of spur dike.

REFERENCES

Launder, B. E. and Spalding, D. B., 1974, "The numerical computation of turbulent flows," Comput. Methods Appl. Mech. Eng., Vol.3, pp.269-289.

Shih, T. H., Zhu, J. and Lumlely, J. L., 1995, "A new Reynolds stress algebraic equation model," Comput. Methods Appl. Mech. Engrg, Vol.125, pp.287-302.

Speziale, C. G. and Thangma, S., 1992, "Analysis of a RNG based turbulence model for separated flows," NASA, CR-189600, ICASE Rept. No. 92-3.

Tominaga, A. and Chiba, S., 1996, "Flow structure around a submerged spur dike," Proc. of Annual Meeting of Japan Society of Fluid Mechanics, pp.317-318 (In Japanese).

Zhu, J. and Shih, T. H., 1994, "Calculations of turbulent separated flows with two-equation turbulence models," J. Computational Fluid Dynamics, Vol.3, pp.343-354.

Hayase, T., Humphrey, J.A.C. and Greif, R., 1992, "A consistently formulated QUICK scheme for fast and stable convergence using finite-volume iterative calculation procedures," Journal of Computational Physics, Vol.98, pp.108-118.